DOI: 10.1002/ejic.200800179

μ-1,3- (*trans*) and μ-1,2- (*cis*) Bonding in Squarato-Bridged Dinuclear Copper(II) and Nickel(II) Complexes Derived from Polypyridyl Amines[‡]

Salah S. Massoud,*[a] Franz A. Mautner,[b] Ramon Vicente,[c] and Febee R. Louka[a]

Keywords: Copper / Nickel / Dinuclear complexes / Squarato bridges / Crystal structures / Magnetic properties

A novel series of dinuclear squarato-bridged copper(II) and nickel(II) complexes $[Cu_2(TPA)_2(\mu_{1,3}\text{-}C_4O_4)](ClO_4)_2\cdot 4H_2O$ (**1**), $[Cu_2(MeDPA)_2(\mu_{1,3}\text{-}C_4O_4)(H_2O)_4](ClO_4)_2$ (**2**) and $[Ni_2(TPA)_2(\mu_{1,2}\text{-}C_4O_4)(H_2O)_2](ClO_4)_2$ (**3**) [$C_4O_4^{2-}$ = dianion of 3,4-dihydroxycyclobut-3-en-1,2-dione (squaric acid), MeDPA = *N*-methylbis(2-pyridylmethyl)amine, TPA = tris(2-pyridylmethyl)amine] were synthesized and structurally characterized by X-ray crystallography. The spectral and structural characterizations as well as their magnetic properties are reported. In this series, the structures consist of the ClO_4^- groups as counterions and the $C_4O_4^{2-}$ anions bridging the two M^{II} centers in a μ-1,3- (**1** and **2**) or in a μ-1,2-bis(monodentate) (**3**) bonding fashion. The coordination geometry around the five-coordinate Cu^{II} centers in **1** is a distorted trigonal bipyramid, where the coordination environment is achieved by the four N-donor atoms of the TPA ligand and one oxygen atom of the bridging squarato ligand. The complexes **2** and **3** adopt a distorted octahedral geometry. The six-coordinate 4+2 environment in **2** is achieved by the three N-atoms of the MeDPA ligand, by an oxygen atom of a bridging squarato ligand and, at longest distances, by two oxygen atoms from coordinated water molecules. In the nickel complex **3**, the geometry is attained by the four N-atoms of TPA and by two oxygen atoms supplied by a coordinated water molecule and by a bridging squarato ligand. The results manifested the effects of the blocking amine variations on the structure and on the bonding mode of the bridging squarato ligand. The complexes show antiferromagnetic coupling with $|J|$ = 9.1 and 1.2 cm^{-1} in the μ-1,3-bridged squarato compounds **1** and **2**, and with J = –1.4 cm^{-1} in the corresponding μ-1,2-bridged squarato complex **3**. The magnetic properties are discussed in relation to other related compounds and the structural data.

Introduction

The highly symmetrical nature and the extensive π-electron delocalization of the cyclic squarate dianion, $C_4O_4^{2-}$ (3,4-dihydroxycyclobut-3-ene-1,2-dionate), where its four C–O bonds have partial double-bond character, made its interaction with metal ions to be an interesting attractive topic for a number of studies in the last two decades.[1–25] The presence of four donor oxygen atoms and the richness of the electron density on the squarate dianion enhance its capability to simultaneously bind more than one metal ion, hence acting as a bridging ligand.[1–25] The bridging squarato ligand affords three types of coordination modes known as μ-1,3- (*trans*),[2–4,6,16,22] μ-1,2- (*cis*),[2,5,8,9,13,14,16,18] and μ-1,2,3,4-.[7,19] Polymeric structures via μ-1,2- and μ-1,3-coordination have also been reported.[11,12,22,25] More recently, the trinuclear complex, $[Cu_3(pmap)_3(\mu_{1,2,3}\text{-}C_4O_4)](ClO_4)_4\cdot 2H_2O$ {pmap = bis[2-(2-pyridyl)ethyl][(2-pyridyl)methyl]amine} with the μ-1,2,3-coordination mode has been structurally and magnetically characterized.[1] The different bonding modes in squarato-bridged metal(II) complexes are depicted in Scheme 1. The bonding modes in these complexes are most likely determined by the geometrical and the structural nature of the blocking ligands coordinated to the central metal ion. In the squarato-bridged M^{II} complexes, the intradimer separation distances between the metal centers vary from ca. 5 Å in the *cis*- (μ-1,2) bonding to 8 Å in the *trans*- (μ-1,3) bonding.[1–25]

The magnetic measurements on structurally characterized squarato-bridged dinuclear nickel(II) and copper(II) complexes reveal weak antiferromagnetic interactions between the paramagnetic centers[2,4,18] ($|J|$ = 0.4–1.7 cm^{-1} in Ni^{II} and $|J|$ = 0–26 cm^{-1}for Cu^{II} complexes, J is the singlet–triplet exchange constant). In general, the dinuclear copper(II) complexes with the μ-1,3-squarato bonding are usually antiferrromagnetically coupled with $|J|$ values in the range of 0–8.6 cm^{-1}.[2,5,10,14,18] The μ-1,2-squarato-bridged compounds show higher $|J|$ values[2,16,10,14,18] in the range

---

[‡] Squarato-Metal(II) Complexes, 3. Part 2: Ref.[1]

[a] Department of Chemistry, University of Louisiana at Lafayette,
P. O. Box 44370, Lafayette, LA 70504, USA
Fax: +01-337-482-5676
E-mail: ssmassoud@louisiana.edu

[b] Institut für Physikalische and Theoretische Chemie, Technische Universität Graz,
8010 Graz, Austria
E-mail: mautner@ptc.tu-graz.ac.at

[c] Departament de Química Inorgànica, Universitat de Barcelona,
Diagonal 647, 08028 Barcelona, Spain
E-mail: ramon.vicente@qi.ub.es

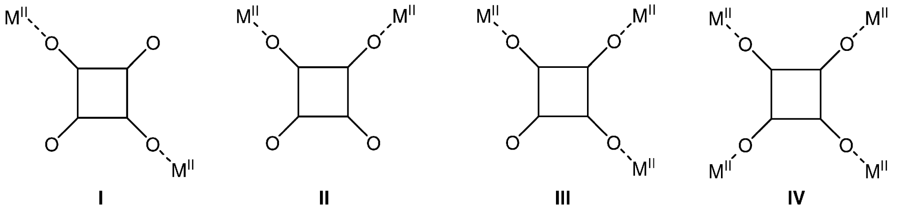

Scheme 1.

of 10.3–26.4 cm^{-1}. This was attributed to the large delocalization in the SOMOs of μ-1,2-squarato compounds compared to those of μ-1,3-squarato compounds.[16] Aside from this trend, very weak ferromagnetic interaction has been reported in $[Cu_2(bpcam)_2(\mu_{1,3}\text{-}C_4O_4)(H_2O)_4]\cdot 10H_2O$ [bpcam = bis(2-pyrimidyl)amidate].[4] In this compound, a *J* value of 1.3 cm^{-1} was interpreted on the basis of accidental orthogonality of magnetic orbitals.[4]

In a continuous effort to understand the factors that might affect the coordination mode of bonding in the squarato-bridged metal(II) complexes and how this is related to the magnetic exchange pathways in theses complexes, the present study was undertaken to explore the structural and magnetic properties of a novel series of dinuclear squarato-bridged Cu^{II} and Ni^{II} compounds based on polypyridylamine ligands. The structures of these ligands and their abbreviations are illustrated in Scheme 2.

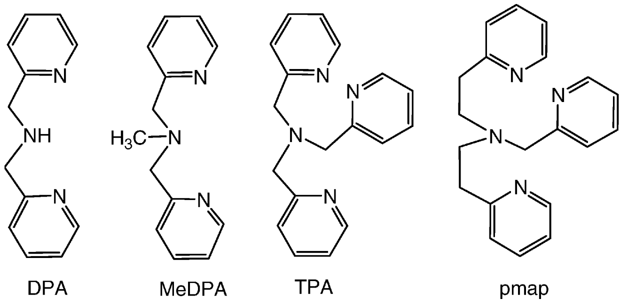

Scheme 2.

Results and Discussion

Synthesis of the Complexes

The dinuclear squarato-bridged complexes $[Cu_2(TPA)_2(\mu_{1,3}\text{-}C_4O_4)](ClO_4)_2\cdot 4H_2O$ (**1**), $[Cu_2(MeDPA)_2(\mu_{1,3}\text{-}C_4O_4)(H_2O)_4](ClO_4)_2$ (**2**) and $[Ni_2(TPA)_2(\mu_{1,2}\text{-}C_4O_4)(H_2O)_2](ClO_4)_2$ (**3**) were synthesized in reasonably good yield (50–80%) by the direct reaction of an aqueous or a methanolic solution of the preformed 1:1 complex $M(ClO_4)_2$/polypyridylamine (M = Cu^{II} or Ni^{II}; polypyridylamine = TPA, MeDPA) and 1 equiv. of disodium squarate. Crystals suitable for X-ray analysis were obtained by slow evaporation of the solvent from dilute aqueous solutions at room temperature. The synthesized complexes were characterized by elemental analyses, and IR and UV/Vis spectroscopy as well as X-ray structure determination.

Infrared Spectroscopy

The infrared spectra of the squarato complexes under investigation display some common features characteristic to the coordinated and uncoordinated water molecules over the range 3420–3450 cm^{-1} and to the presence of hydrogen bonding (3600–3350 cm^{-1}). The perchlorate ions display strong bands over the range 1086–1121 cm^{-1}. The broadening or the split of the perchlorate band in these complexes most probably results from the reduction of the symmetry of the ClO_4^- ion to C_{3v} or to C_{2v}. It may also be attributed to the interaction of the ClO_4^- ions with the lattice water in **1** or with aqua water molecules in **2** and **3** (see Crystal Structure section). The IR spectra of the complexes also display strong to medium intensity bands in the 1550–1440 cm^{-1} region. The strong band observed around 1500 cm^{-1} is similar to that found in the spectrum of $K_2C_4O_4$ which has been tentatively assigned to a mixture of C–O and C–C stretching vibration modes.[7,26,27] In the squarato-bridged metal complexes, it has been shown that the position of the 1500 cm^{-1} band cannot be used as a diagnostic tool to distinguish between the coordination modes of $\mu_{1,2}$- and $\mu_{1,3}$-bis(monodentate ligand).[2,18] This was attributed to the strong influence of the blocking ligand and to the structural environment around the bridging squarato moiety.[2,18]

Electronic Spectra

The visible spectra of the dinuclear squarato-bridged Cu^{II} complexes **1** and **2** were recorded in MeOH and in other solvents (Table 1). The complexes reveal strong absorption maxima in the 410–500 nm region which can most probably be attributed to a CT (L → M) transition. In MeOH and/or H_2O, complex **1** displays absorption maxima at 860 and a high-energy shoulder at 655 nm. The spectral features of **1** are consistent with the five-coordinate geometry around the Cu^{II} centers which are characterized by a rather broad d–d absorption band in their solution electronic spectra. Cu^{II} complexes with trigonal-bipyramidal (TBP) geometries, generally exhibit a maximum at $\lambda >$ 800 nm (d_{xy}, $d_{x^2-y^2} \rightarrow d_{z^2}$) with a higher energy shoulder (spin-forbidden, d_{xz}, $d_{yz} \rightarrow d_{z^2}$).[28–30] In contrast, square-pyramidal or distorted square-pyramidal (SP) Cu^{II} complexes usually show a band in the 550–660 nm range (d_{xz}, $d_{yz} \rightarrow d_{x^2-y^2}$).[2,30,31] Inspection of the electronic spectroscopic data shown in Table 1 and on the basis of the above criterion, in solution complex **1** adapts a TBP stereochemis-

Table 1. Visible spectroscopic data [λ_{max}/nm (ε_{max}/M^{-1}cm^{-1})] for the (bridging squarato)Cu^{II} complex ions in different solvents.

Solvent	$[Cu_2(TPA)_2(\mu_{1,3}\text{-}C_4O_4)]^{2+}$	$[Cu_2(MeDPA)_2(\mu_{1,3}\text{-}C_4O_4)(H_2O)_4]^{2+}$
H_2O	439 (364), ca. 655 (163), 860 (448)	409 (400), 648 (247)
MeOH	461 (1030), 656 (211), 860 (220)	431 (1440), 600 (454)
CH_3CN	497 (2930), ca. 661 (596), 870 (488)	
CH_3NO_2	492 (2490), ca. 664 (508), 870 (479)	

try. On the other hand, the very broad single absorption band observed in the solution spectrum of **2** is most likely consistent with an octahedral geometry around the central Cu^{2+} ion.

The visible spectrum of the aqueous solution of $[Ni_2(TPA)_2(\mu_{1,2}\text{-}C_4O_4)(H_2O)_2](ClO_4)_2$ (**3**) displays three bands at 577, 776 and 860 nm. These features are consistent with a six-coordinate octahedral geometry.[2,33,39] Thus, the solution spectrum of the complex ion is adequately explained by d–d transitions in the distorted octahedral environment of the Ni^{II} ion, where the absorption maxima result from $^3A_{2g} \rightarrow {}^3T_{1g}(P)$, $^3A_{2g} \rightarrow {}^3T_{1g}(F)$ and $^3A_{2g} \rightarrow {}^3T_{2g}(F)$ transitions.

The trigonal-bipyramidal environment around the central Cu^{2+} ion in $[Cu_2(TPA)_2(\mu_{1,3}\text{-}C_4O_4)](ClO_4)_2\cdot 4H_2O$ (**1**) was observed in many of the Cu^{II} and Co^{II} complexes derived from aliphatic tripod tetraamines or from TPA.[28,29,31–37] Increasing of the length of the pyridyl arms in TPA to pmap as in $[Cu_3(pmap)_3(\mu_{1,2,3}\text{-}C_4O_4)](ClO_4)_4\cdot 2H_2O$ (see Scheme 2) was associated with a stereochemical change of the central Cu^{II} ion to a distorted square-pyramidal configuration.[1] Similar results were reported on going from $[Cu(TPA)X]ClO_4$ (X = Cl^-, N_3^-, NO_2^- and NCS^-) to $[Cu(pmea)Cl]ClO_4$ {pmea = [2-(2-pyridyl)ethyl]bis(2-pyridylmethyl)amine} and $[Cu(pmap)Cl]ClO_4$.[28,32,38] The visible spectra of the green complex **1** in CH_3CN or in CH_3NO_2 were slightly shifted to longer wavelengths (Table 1), and the dissolution was accompanied by a color change to purple/wine red, which most likely can be attributed to the displacement of one of the Cu–O(squarate) bonds by a solvent molecule in order to relieve the steric hindrance around the coordinated squarato ligand.[1]

Crystal Structures

$[Cu_2(TPA)_2(\mu_{1,3}\text{-}C_4O_4)](ClO_4)_2\cdot 4H_2O$ (1)

The ORTEP drawing for **1** and atom labeling scheme are illustrated in Figure 1a, and selected bond parameters are given in Table 2. The structure of the compound consists of centrosymmetric dinuclear units in which the copper atoms are linked by the squarate dianion in a $\mu_{1,3}\text{-}C_4O_4$ bonding fashion, perchlorate counterions and lattice water molecules. The copper atom is pentacoordinate in a distorted coordination polyhedron close to a trigonal bipyramid (τ = 0.89).[40] Three pyridyl nitrogen atoms of the TPA ligand determine the equatorial plane of Cu(1) polyhedra with Cu–N$_{py}$ bond lengths in the 2.062(4)–2.075(4) Å range. The axial coordination sites are occupied by an oxygen atom O(1) of the bridging squarato ligand and N(1) of the TPA ligand. The Cu(1)–O(1) and Cu(1)–N(1) axial distances are 1.944(3) and 2.005(4) Å, respectively. The copper(II) center deviates by 0.215 Å from its CuN_3 equatorial plane which forms a dihedral angle of 86.3° with the plane of the bridging squarato ligand. The Cu(1)–O(1)–C(19) bond angle is 125.7(3)°. The Cu···Cu intradinuclear distance is 7.5807(18) Å, whereas the shortest Cu···Cu interdimer distances are 7.577(18) and 9.234(2) Å. Three hydrogen bonds of the type O–H···O are observed: a non-coordinated oxygen atom O(2) acts as an acceptor for two hydrogen bonds from lattice water molecules O(7) and O(8), and the remaining hydrogen bond is formed between the two lattice water molecules (Figure 1b, Table 5). The pyridine rings of the TPA molecules have ring–ring separations of their centers of gravities (Cg) of more than 4.40 Å.

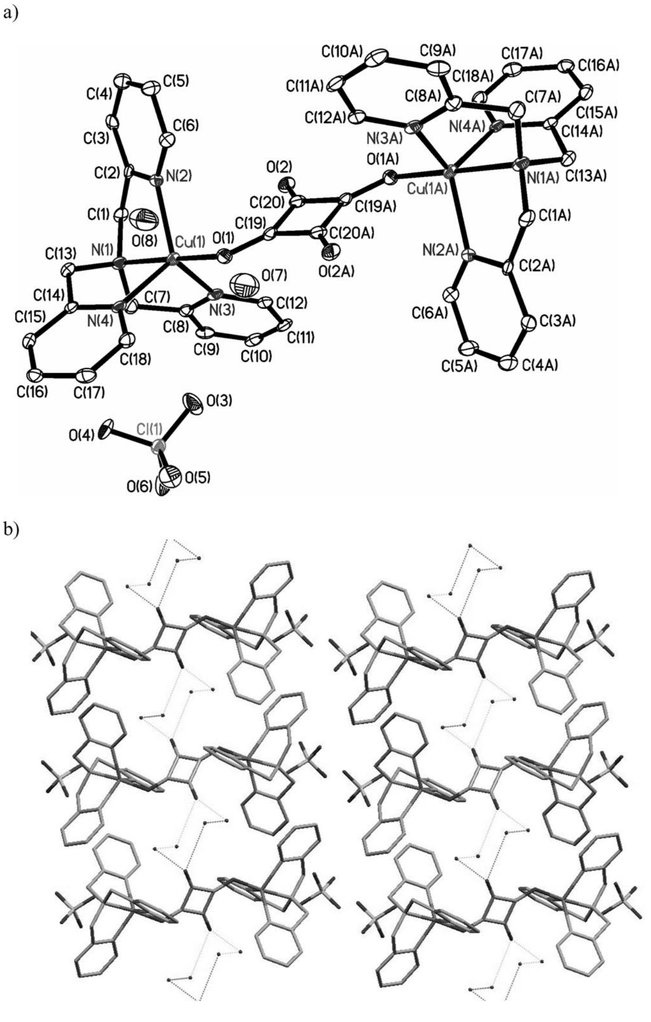

Figure 1. (a) Molecular geometry and atom labeling scheme of **1**. (b) Packing view of **1**.

Table 2. Selected bond lengths [Å] and angles [°] for **1**.[a]

Cu(1)···Cu(1A)	7.5807(19)	Cu(1)–O(1)	1.944(3)
Cu(1)–N(1)	2.005(4)	Cu(1)–N(2)	2.062(4)
Cu(1)–N(3)	2.064(4)	Cu(1)–N(4)	2.075(4)
O(1)–C(19)	1.269(6)	O(2)–C(20)	1.247(6)
C(19)–C(20A)	1.464(7)	C(19)–C(20)	1.472(7)
O(1)–Cu(1)–N(1)	174.8(2)	O(1)–Cu(1)–N(2)	98.2(2)
N(1)–Cu(1)–N(2)	82.3(2)	O(1)–Cu(1)–N(3)	101.7(2)
N(1)–Cu(1)–N(3)	82.2(2)	N(2)–Cu(1)–N(3)	121.5(2)
O(1)–Cu(1)–N(4)	93.7(2)	N(1)–Cu(1)–N(4)	81.5(2)
N(2)–Cu(1)–N(4)	116.7(2)	N(3)–Cu(1)–N(4)	116.1(2)
O(1)–C(19)–C(20A)	132.5(5)	O(1)–C(19)–C(20)	136.5(5)
C(20A)–C(19)–C(20)	91.0(4)	O(2)–C(20)–C(19A)	135.1(5)
O(2)–C(20)–C(19)	135.8(5)	C(19A)–C(20)–C(19)	89.0(4)

[a] Symmetry code: (A): –*x*, –*y* + 1, –*z*.

$[Cu_2(MeDPA)_2(\mu_{1,3}\text{-}C_4O_4)(H_2O)_4](ClO_4)_2$ (2)

A labeled ORTEP drawing of compound **2** is shown in Figure 2a, and selected bond parameters are given in Table 3. The structure of the compound consists of centrosymmetric dinuclear units in which the copper atoms are bridged by a $\mu_{1,3}$-C_4O_4 ligand, and perchlorate counterions. Each copper atom has an elongated octahedral coordination geometry. The CuN_3O_3 chromophore is achieved by the three N atoms of the tridentate MeDPA blocking ligand, and by three oxygen atoms, namely O(1) of a $\mu_{1,3}$-C_4O_4 ligand, and O(3) and O(4) of two aqua ligands. The equatorial plane is formed by O(1), N(1), N(2), N(3) and Cu(1) atoms, whereas the axial sites are occupied by O(3) and O(4). The equatorial Cu(1)–O(1) bond length is 1.960(3) Å, and the Cu(1)–N bonds are in the range from 1.987(4) to 2.039(4) Å. The bond angles in the equatorial plane are in the 82.28(14)–99.88(14)° range. The axial Cu(1)–O(3) and Cu(1)–O(4) bonds are 2.381(3) and 2.434(4) Å, respectively, and the O(3)–Cu(1)–O(4) bond angle is 170.01(12)°. The Cu(1) center deviates by 0.206 Å, whereas C(2) deviates by 0.006 Å from the mean plane of the bridging squarato ligand which forms an interplanar angle with the plane of the equatorial CuN_3O plane of 71.6°. The Cu(1)–O(1)–C(1) bond angle is 140.1(3)°. Bond parameters of the squarato dianion are comparable with the corresponding values reported in complex **3** (see next). The Cu···Cu intradinuclear distance is 7.997(2) Å, and the shortest Cu···Cu interdimer distances are 6.2718(17) and 8.232(2) Å. Hydrogen bonds of the type O–H···O (Table 5, Figure 2b) connect the dinuclear units and the ClO_4^- counterions to form a supramolecular 2D network extended along the *a*- and *b*-axis of the unit cell. The pyridine rings of adjacent MeDPA molecules have the following ring–ring separations of their centers of gravities (Cg): Cg(N2)···Cg(N2)#B = 3.875(4) Å [#B: 2 – *x*, 1 – *y*, 1 – *z*]; Cg(N3)···Cg(N3)#C = 3.752(4) Å [#C: 2 – *x*, 1 – *y*, –*z*]; (N2): ring N(2),C(11)–C(15); N(3): ring N(3),C(3)–C(7).

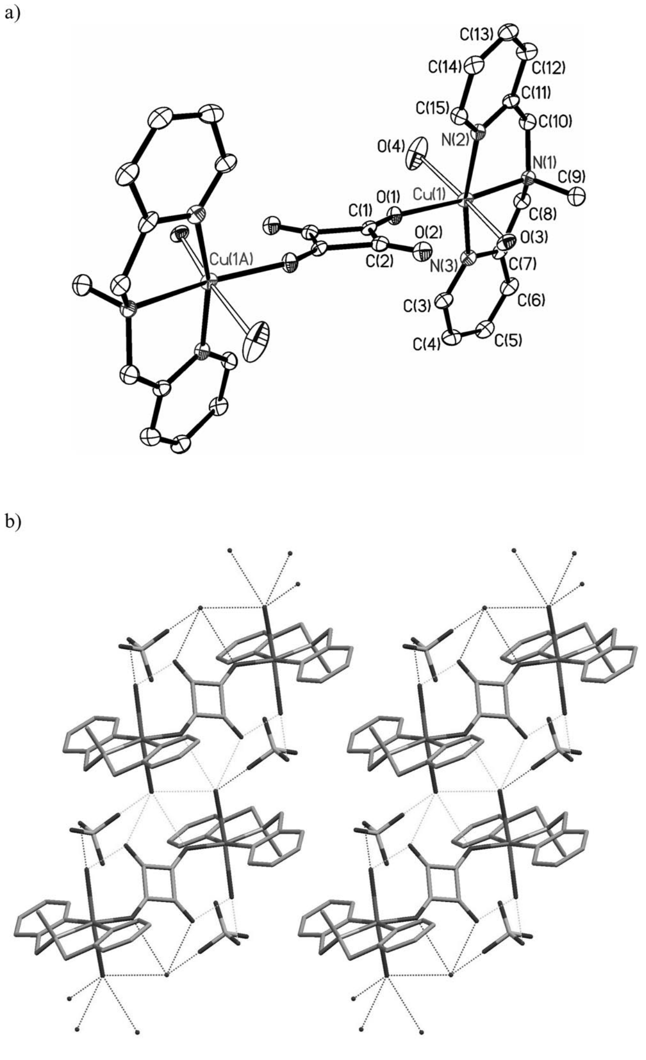

Figure 2. (a) Molecular geometry and atom labeling scheme of the dinuclear cation of **2**. (b) Packing view of **2**.

Table 3. Selected bond lengths [Å] and angles [°] for **2**.[a]

Cu(1)···Cu(1A)	7.997(2)	Cu(1)–O(1)	1.960(3)
Cu(1)–N(3)	1.987(4)	Cu(1)–N(2)	1.987(4)
Cu(1)–N(1)	2.039(4)	Cu(1)–O(3)	2.381(3)
Cu(1)–O(4)	2.434(4)	O(1)–C(1)	1.243(5)
O(2)–C(2)	1.223(5)	C(1)–C(2)	1.464(6)
C(1)–C(2A)	1.483(6)		
O(1)–Cu(1)–N(3)	94.57(14)	O(1)–Cu(1)–N(2)	99.88(14)
N(3)–Cu(1)–N(2)	165.0(2)	O(1)–Cu(1)–N(1)	167.60(12)
N(3)–Cu(1)–N(1)	82.8(2)	N(2)–Cu(1)–N(1)	82.28(14)
O(1)–Cu(1)–O(3)	92.50(11)	N(3)–Cu(1)–O(3)	97.00(12)
N(2)–Cu(1)–O(3)	86.22(12)	N(1)–Cu(1)–O(3)	99.83(12)
O(1)–Cu(1)–O(4)	80.32(14)	N(3)–Cu(1)–O(4)	90.55(14)
N(2)–Cu(1)–O(4)	88.16(14)	N(1)–Cu(1)–O(4)	87.57(14)
O(3)–Cu(1)–O(4)	170.01(12)	C(1)–O(1)–Cu(1)	140.1(3)
O(1)–C(1)–C(2)	137.4(4)	O(1)–C(1)–C(2A)	131.5(4)
C(2)–C(1)–C(2A)	91.2(3)	O(2)–C(2)–C(1)	136.1(4)
O(2)–C(2)–C(1A)	135.0(4)	C(1)–C(2)–C(1A)	88.8(3)

[a] Symmetry code: (A): –*x* + 2, –*y* + 1, –*z*.

$[Ni_2(TPA)_2(\mu_{1,2}\text{-}C_4O_4)(H_2O)_2](ClO_4)_2$ (3)

A labeled ORTEP plot for compound **3** is shown in Figure 3a, and selected bond parameters are given in Table 4. The structure of the compound consists of $[C_{40}H_{40}N_8Ni_2O_6]^{2+}$ dinuclear units in which the nickel atoms are bridged by the $\mu_{1,2}$-C_4O_4 ligand, and perchlorate counterions. Each nickel atom has a slightly distorted octahedral coordination geometry. The octahedron around the Ni^{2+} centers is achieved by the four N-atoms of the tetradentate amine, TPA, with Ni–N bond lengths in the 2.074(3)–2.102(3) Å range. The remaining sites of the Ni^{2+} polyhedra are occupied by two *cis*-coordinated oxygen atoms, O(1) of the squarate ligand, and O(3) of an aqua ligand. The Ni–O(1) bond is shorter [2.052(2) Å] than the Ni–O(3) bond [2.058(2) Å]. The Ni···Ni intradinuclear distance is 7.2812(17) Å, and the shortest Ni···Ni interdimer distances are 8.0150(18) and 8.3009(18) Å. The central squarato anion is located on a twofold rotation axis and acts as $\mu_{1,2}$-bridging ligand within the dinuclear unit. The Ni(1) center deviates by 0.1330 Å, whereas O(2) deviates by 0.062 Å from the mean plane of the squarato ligand. The bridging squarato ligand forms an interplanar angle of 21.9° with the NiN_2O_2 [i.e.: Ni(1), O(1), O(3), N(1), N(4)] plane. The Ni(1)–O(1)–C(19) bond angle is 132.2(2)°. Hydrogen bonds of the type O–H···O are formed from aqua ligand O(3) to the non-coordinated oxygen atom of the squarate anion O(2) and perchlorate oxygen atom O(4) (Table 5, Figure 3b).

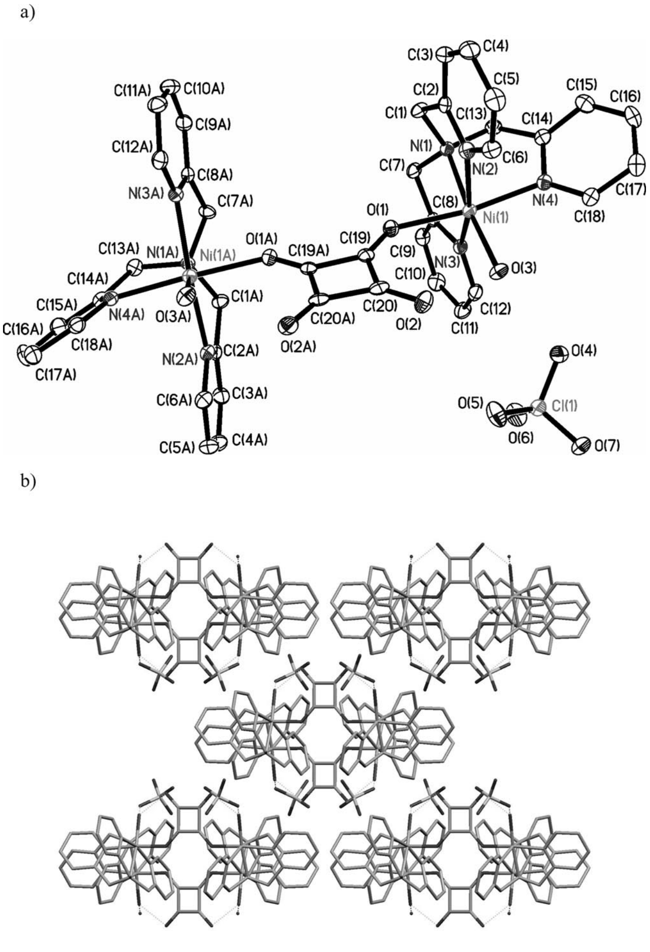

Figure 3. (a) ORTEP view and atom labeling scheme of **3**. (b) Packing view of **3**.

Table 4. Selected bond lengths [Å] and angles [°] for **3**.[a]

Ni(1)···Ni(1A)	7.2812(17)	Ni(1)–O(3)	2.052(2)
Ni(1)–O(1)	2.058(2)	Ni(1)–N(4)	2.074(3)
Ni(1)–N(3)	2.077(3)	Ni(1)–N(1)	2.083(3)
Ni(1)–N(2)	2.102(3)	O(1)–C(19)	1.256(4)
O(2)–C(20)	1.247(4)	C(19)–C(19A)	1.461(6)
C(19)–C(20)	1.476(4)	C(20)–C(20A)	1.474(6)
O(3)–Ni(1)–O(1)	94.82(9)	O(3)–Ni(1)–N(4)	92.02(10)
O(1)–Ni(1)–N(4)	172.15(10)	O(3)–Ni(1)–N(3)	102.50(10)
O(1)–Ni(1)–N(3)	86.15(10)	N(4)–Ni(1)–N(3)	96.13(10)
O(3)–Ni(1)–N(1)	174.85(10)	O(1)–Ni(1)–N(1)	89.57(9)
N(4)–Ni(1)–N(1)	83.43(10)	N(3)–Ni(1)–N(1)	80.45(10)
O(3)–Ni(1)–N(2)	95.87(10)	O(1)–Ni(1)–N(2)	90.47(10)
N(4)–Ni(1)–N(2)	85.00(10)	N(3)–Ni(1)–N(2)	161.53(10)
N(1)–Ni(1)–N(2)	81.37(10)	C(19)–O(1)–Ni(1)	132.2(2)
O(1)–C(19)–C(19A)	132.7(2)	O(1)–C(19)–C(20)	137.1(3)
C(19A)–C(19)–C(20)	90.2(2)	O(2)–C(20)–C(20A)	135.6(2)
O(2)–C(20)–C(19)	134.6(3)	C(20A)–C(20)–C(19)	89.7(2)

[a] Symmetry code: (A): –*x* + 1, *y*, –*z* + 3/2.

Table 5. Selected hydrogen bonds in complexes **1**–**3**.

D–H···A[a]	D···A [Å]	D–H···A [°]	Symmetry code of A
Complex **1**			
O(7)–H(71)···O(8)	2.961(7)	172.2	
O(7)–H(72)···O(2)	2.877(5)	177.1	–*x*, 1 –*y*, –*z*
O(8)–H(82)···O(2)	2.854(6)	159.2	*x*, 1/2 – *y*, 1/2 + *z*
Complex **2**			
O(3)–H(31)···O(2)	2.730(4)	167.2	
O(3)–H(32)···O(5)	2.993(7)	150.8	1 + *x*, 1 + *y*, *z*
O(4)–H(41)···O(1)	3.005(5)	137.6	1 – *x*, 1 – *y*, –*z*
O(4)–H(41)···O(4)	2.965(7)	134.9	1 – *x*, 1 – *y*, –*z*
O(4)–H(42)···O(6)	2.932(7)	169.4	
Complex **3**			
O(3)–H(31)···O(2)	2.609(4)	175.6	
O(3)–H(32)···O(4)	2.831(4)	169.3	

[a] D = Donor, A = acceptor.

Although in complexes **1**–**3** only two of the four oxygen atoms in each of the bridging squarato dianions are coordinated to metal ions, the symmetry of the geometrical arrangement of the squarato ligands, remains unchanged. In these complexes, the bond lengths of the squarato ligands are: C–O 1.223(5)–1.269(6) Å, C–C 1.461(6)–1.483(6) Å; the C–C–C bond angles [88.8(3)–91.2(3)°] are close to 90°, and the O–C–C bond angles of non-coordinated oxygen atoms are close to 135° [134.6(3)–136.1(4)°], whereas the corresponding O–C–C bond angles of the coordinated oxygen atoms reveal more asymmetric behavior: 132.5(5) and 136.5(5)° for **1**, 131.5(4) and 137.4(4)° for **2**, and 132.7(2) and 137.1(3)° for **3**.

Hydrogen bonds are also observed in the title complexes (Table 5): In **1**, the uncoordinated oxygen atom O(2) acts as an acceptor for two hydrogen bonds of the type O–H···O with lattice water molecules O(7) and O(8) [O(7)–H(72)···O(2) (–*x*, 1 – *y*, –*z*): O(7)···O(2) = 2.877(5) Å, O(7)–H(72)···O(2) = 177.1°; O(8)–H(82)···O(2) (*x*, 1/2 – *y*, 1/2 – *z*): O(8)···O(2) = 2.854(6) Å, O(8)–H(82)···O(2) = 159.2°]. In **2** and **3**, the uncoordinated oxygen atoms O(2) act as acceptors for a strong hydrogen bond of the type O–H···O with lattice water molecules O(3) [**2**: O(3)–H(31)···O(2): O(3)···O(2) = 2.730(4) Å, O(3)–H(31)···O(2) = 167.2°; **3**: O(3)–H(31)···O(2): O(3)···O(2) = 2.609(4) Å, O(3)–H(31)···O(2) = 175.6°]. The data presented above concerning the bridging squarato centers agree well with those reported by Robl et al. based on X-ray and neutron diffraction measurements performed on a series of (squarato)metal hydrates.[41] These studies revealed that the non-coordinated oxygen atoms of the squarato ligands are involved in strong hydrogen bonds, thus compensating the electronic effects of the metal coordination to the remaining oxygen atoms of the central squarato ligands.

Magnetic Properties

Variable-temperature (2–300 K) magnetic susceptibility data were collected on polycrystalline samples for **1**–**3**. The magnetic behavior of the copper(II) compounds **1** and **2** is represented in Figure 4 in the forms of χ_M vs. T plots. At 300 K, the χ_M value for compound **1** is 3×10^{-3} cm^{3}mol^{-1}. Upon cooling, χ_M increases gradually to arrive at a maximum of 0.051 cm^{3}mol^{-1} at 3 K, and then it decreases to a value of 0.014 cm^{3}mol^{-1} at 2 K. Such a behavior reveals an intramolecular antiferromagnetic interaction. On the basis of this situation, the experimental magnetic data have been fitted by using the expression derived through the Hamiltonian $\hat{H} = -J\hat{S}_A\cdot\hat{S}_B$ with $S_A = S_B = 1/2$ [Equation (1)].

$$\chi_M = (2Ng^2\mu_B{}^2/kT)\{[\exp(J/kT)]/[1 + 3\exp(J/kT)]\} \qquad (1)$$

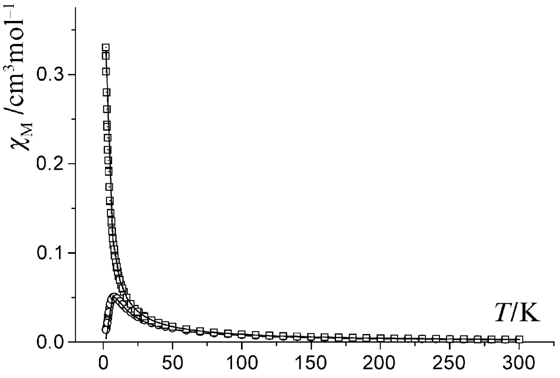

Figure 4. Temperature dependence of χ_M of solid samples of complexes **1** (open circles) and **2** (open squares). The solid lines represent the best fit (see text).

The parameters N, μ_B and k in Equation (1) have their usual meanings. Least-squares fitting of all experimental data leads to the parameters $J = -8.2$ cm^{-1} and $g = 2.02$. In case of compound **2**, the χ_M value at 300 K is 3×10^{-3} cm^{3}mol^{-1}. Upon cooling, it increases continuously to arrive at a value of 0.321 cm^{3}mol^{-1} at 2 K (Figure 4). The absence of a maximum before 2 K in the χ_M vs. T plot for **2** indicates a small or non-existing J coupling. Based on this situation, the experimental magnetic data have been fitted by using Equation (1). Least-squares fitting of all experimental data leads to $J = -1.2$ cm^{-1} and $g = 2.16$.

From the structural point of view, two factors may be considered to account for the different antiferromagnetic coupling between **1** and **2**. These include the magnetic orbitals and Cu–O–C bond angles. In **1**, the Cu^{II} centers show a trigonal-bipyramidal geometry and consequently, a d_{z^2} orbital is the "magnetic orbital". In **2**, the Cu^{II} cations adopt a 4+2 octahedral coordination (the water molecules have long Cu···O distances of 2.381(3) and 2.434(4) Å] where the "magnetic orbital" $d_{x^2-y^2}$ is perpendicular to the squarato plane with one of its lobes oriented towards an oxygen atom of the squarato ligand. Therefore, it should be expected that the interaction in complex **1** occurs through the d_{z^2} orbital which should lead to more antiferromagnetic coupling than that observed in **2** due to a larger overlap between magnetic orbitals.[1,19] Complexes **1** and **2** show the same *syn* conformation[1] with respect to the squarato bridging ligand. For this conformation, increasing of the Cu–O–C angle values, diminishes the antiferromagnetic coupling.[1] The Cu–O–C angles for **1** and **2** are 125.6 and 140.12°, respectively.

The magnetic behavior of the nickel(II) compound **3** is represented in Figure 5 in the form of a $\chi_M T$ vs. T plot. At 300 K, the $\chi_M T$ product is 2.43 cm^3 K mol^{-1}. This value, as usual for Ni^{II} ions ($g > 0$), is larger than those expected for two uncoupled S = 1 spins (1.98 cm^3 K mol^{-1}, $g = 2.0$). Upon cooling, $\chi_M T$ remains nearly constant, and it decreases clearly from approximately $T < 25$ K indicating antiferromagnetic coupling. At 2 K, the $\chi_M T$ value is 0.94 cm^3 K mol^{-1}. The corresponding χ_M vs. T plot for **3** increases on cooling and exhibits no maximum over the temperature range studied. The experimental magnetic data have been fitted by using the expression derived through the Hamiltonian $\hat{H} = -J\hat{S}_A\cdot\hat{S}_B$ with $S_A = S_B = 1$ [Equation (2)].

$$\chi_M = (2Ng^2\mu_B{}^2/kT)\{[\exp(J/kT) + 5\exp(3J/kT)]/[1 + 3\exp(J/kT) + 5\exp(3J/kT)]\} \qquad (2)$$

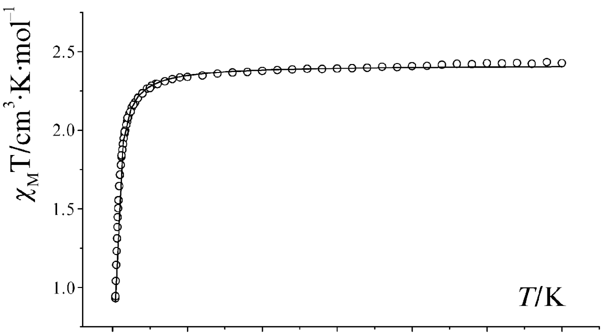

Figure 5. Temperature dependence of $\chi_M T$ of a solid sample of complex **3**. The solid line represents the best fit (see text).

Least-squares fitting of all experimental data leads to the parameters $J = –1.43\ \mathrm{cm}^{-1}$ and $g = 2.20$. Only one μ-1,2-squarato dinuclear $\mathrm{Ni^{II}}$ compound with a J value of $–0.4\ \mathrm{cm}^{-1}$ had been reported.[13]

Conclusions

From the synthetic point of view it can be pointed out that a small alteration in the ligand skeleton such as methylation of the secondary amine nitrogen atom of DPA in the complex $[Cu_2(DPA)_2(\mu_{1,2}\text{-}C_4O_4)(H_2O)_2](ClO_4)_2$[2] to produce MeDPA $\{[Cu_2(MeDPA)_2(\mu_{1,3}\text{-}C_4O_4)(H_2O)_4](ClO_4)_2$ (**2**)} resulted in a change of the bonding mode of the bridging squarato ligand from μ-1,2 to μ-1,3 coordination. Moreover, when methylene groups were inserted into the pyridyl arms of the TPA ligand to generate the pmap ligand (Scheme 2), a drastic change was observed, and the tricopper complex $[Cu_3(pmap)_3(\mu_{1,2,3}\text{-}C_4O_4)](ClO_4)_4{\cdot}2H_2O$ was obtained with a μ-1,2,3-squarato coordination mode[1] instead of the μ-1,3 bonding in **1**. This skeletal alteration was accompanied by a stereochemical change around the central Cu^{2+} ion from distorted TBP to distorted SP geometry.[1] Change of the bonding coordination mode of the bridging squarato ligand was also observed when the Cu^{2+} ion in **1** was replaced by Ni^{2+} $\{[Ni_2(TPA)_2(\mu_{1,2}\text{-}C_4O_4)(H_2O)_2](ClO_4)_2$ (**3**)}.

In general, the present study demonstrates that when squarate is acting as a bridging ligand, increasing of the steric hindrance in the blocking amine ligand and/or increasing of the flexibility of its arms tends to stabilize the μ-1,3 bonding. Also, the dinuclear (μ-1,3- or μ-1,2-bridging squarato)metal(II) complexes usually exhibit weak antiferromagnetic interaction. The coupling through the squarato bridging ligand in polynuclear copper(II) complexes has been recently studied.[1] The number of squarato-bridged nickel(II) complexes is still small, and no theoretical studies have been made yet on such systems.

Experimental Section

Materials: The compounds 2-(2-aminoethyl)pyridine, 2-picolyl chloride hydrochloride, methylamine (40% by weight in water) and 3,4-dihydroxy-3-cyclobutene-1,2-dione (squaric acid, $H_2C_4O_4$) were purchased from Aldrich Chem. Co., USA. Bis(2-pyridylmethyl)amine (DPA) was obtained from TCI-America. All other materials were of reagent-grade quality.

Physical Methods: IR spectra were recorded with a JASCO FT/IR-480 plus spectrometer as KBr pellets. Electronic spectra were recorded with an Agilent 8453 HP diode UV/Vis spectrophotometer. Elemental analyses were performed at the Atlantic Microlaboratory, Norcross, Georgia, USA. Magnetic susceptibility measurements for the complexes under a magnetic field of 1 Tesla in the range 2–300 K and magnetization measurements in the field range 0–5 T at 2 K were performed with a Quantum Design MPMS-XL SQUID magnetometer at the Magnetochemistry Service of the University of Barcelona. All measurements were performed on polycrystalline samples. Pascal's constants were used to estimate the diamagnetic corrections which were subtracted from the experimental susceptibilities to give the corrected molar magnetic susceptibilities.

Synthesis of the Ligands and Complexes

Caution! *Salts of perchlorate and their metal complexes are potentially explosive and should be handled with great care and in small quantities.*

Tris(2-pyridylmethyl)amine (TPA): The ligand was synthesized according to the procedures described by Anderegg[42] and modified by Karlin's group,[33] and was characterized as reported.[28]

Methylbis(2-pyridylmethyl)amine (MeDPA): MeDPA was synthesized and characterized by using the published procedures,[43] except that tetrahydrofuran was used as a solvent instead of acetonitrile. The ligand was purified by column chromatography by using alumina and eluted with MeOH/ethyl acetate (2:98, v/v) and recrystallized from diethyl ether by using charcoal.

$[Cu_2(TPA)_2(\mu_{1,3}\text{-}C_4O_4)](ClO_4)_2{\cdot}4H_2O$ (1): A methanolic solution of TPA (0.145 g, 0.5 mmol dissolved in 5 mL of MeOH) was added to an aqueous solution of copper(II) perchlorate hexahydrate (0.190 g, 0.5 mmol in 40 mL of H_2O). The resulting blue solution was gently heated in a steam bath for 5 min, followed by the addition of an equimolar amount of disodium squarate (0.082, 0.5 mmol). The mixture was heated in a steam bath for 15 min during which the color turned green. The mixture was filtered through Celite and allowed to crystallize at room temperature. After 5 d, the shiny green crystalline compound which separated was collected by filtration, washed with 2-propanol, then diethyl ether, and air-dried (overall yield: 193 mg, 73%). Crystals of X-ray quality were obtained from dilute solutions. Characterization: $C_{40}H_{44}Cl_2Cu_2N_8O_{16}$ (1090.83): calcd. C 44.04, H 4.07, N 10.27; found C 44.44, H 3.96, N 10.68. Selected IR bands: $\tilde{\nu}$ = 3447 (m) [ν(O–H) stretching], 1552 (vs), 1480 (s), 1438 (m) [ν(CO)], 1086 (vs) [ν(Cl–O) (ClO_4^-)] cm^{-1}.

$[Cu_2(MeDPA)_2(\mu_{1,3}\text{-}C_4O_4)(H_2O)_4](ClO_4)_2$ (2): Disodium squarate was added (0.81 g, 0.50 mmol) to a hot mixture of copper(II) perchlorate hexahydrate (0.378 g, 1 mmol) and methylbis(2-pyridylmethyl)amine (0.186 g, 1 mmol) dissolved in 20 mL of H_2O. The resulting solution was heated for 15 min, filtered through Celite and allowed to crystallize at room temperature. $C_{30}H_{38}Cl_2Cu_2N_6O_{16}$ (936.7): calcd. C 38.58, H 4.09, N 8.97; found C 38.40, H 4.13, N 8.83. Selected IR bands: $\tilde{\nu}$ = 3448 (m, br.) [ν(O–H) stretching], 1524 (vs), 1481 (m), 1446 (m) [ν(CO)], 1111 (s), 1090 (s) [ν(Cl–O) (ClO_4^-) (split)] cm^{-1}.

$[Ni_2(TPA)_2(\mu_{1,2}\text{-}C_4O_4)(H_2O)_2](ClO_4)_2$ (3): The complex was synthesized essentially as described above for its analogous $\mathrm{Cu^{II}}$ complex **1** (yield: 77%). Violet crystals suitable for X-ray were obtained from dilute aqueous solution. $C_{40}H_{40}Cl_2N_8Ni_2O_{14}$ (1045.14): calcd. C 45.97, H 3.86, N 10.72; found C 45.79, H 3.94, N 10.80. Selected IR bands: $\tilde{\nu}$ = 3423 (m) [ν(O–H) stretching], 1500 (vs), 1440 (m) [ν(CO)], 1121 (m) [ν(Cl–O) (ClO_4^-)] cm^{-1}. UV/Vis (H_2O): λ_{max} (ε_{max}) = 377 (267), 577 (76), 776 (71), 860 nm (96 $\mathrm{M}^{-1}\,cm^{-1}$).

Crystal Data Collection and Refinement: The X-ray single-crystal data of compounds **1**–**3** were collected with a Bruker-AXS SMART APEX CCD diffractometer. The crystallographic data, conditions retained for the intensity data collection and some features of the structure refinements are listed in Table 6. Intensities data were collected with graphite-monochromated Mo-K_α radiation (λ = 0.71073 Å). Lorentz-polarization and absorption corrections were made by using the SADABS computer program.[44] The structures were solved by direct methods with the SHELXS-86[45] computer program, and refined by full-matrix least-squares methods on $|F|^2$

Table 6. Crystal data and structure refinement for complexes **1**–**3**.

Compound	**1**	**2**	**3**
Empirical formula	$C_{40}H_{44}Cl_2Cu_2N_8O_{16}$	$C_{15}H_{19}ClCuN_3O_8$	$C_{20}H_{20}ClN_4NiO_7$
Formula mass	1090.83	468.33	522.54
Crystal system	monoclinic	triclinic	monoclinic
Space group	$P2_1/c$	$P\bar{1}$	$C2/c$
a [Å]	16.667(3)	8.625(2)	18.886(4)
b [Å]	9.234(2)	8.915(2)	15.434(3)
c [Å]	14.565(3)	12.522(3)	16.256(3)
α [°]	90	91.07(3)	90
β [°]	97.84(3)	104.19(3)	90
γ [°]	90	103.76(3)	90
V [Å^3]	2220.7(7)	903.6(3)	4209.9(15)
Z	2	2	8
T [K]	100(2)	100(2)	100(2)
Crystal size [mm]	0.30 × 0.22 × 0.14	0.32 × 0.22 × 0.15	0.32 × 0.22 × 0.10
μ [mm^{-1}]	1.160	1.408	1.101
$D_{\text{calcd.}}$ [Mg/m^3]	1.631	1.721	1.649
Collected data	16067	6449	15914
$I > 2\sigma(I)$	3330	2646	3730
Parameters	319	260	304
R [$I > 2\sigma(I)$]	0.0716	0.0857	0.0502
$wR2$ (all data)	0.1560	0.2473	0.1081
Residual max/min electron density [eÅ^{-3}]	0.625/–0.741	1.174/–1.013	0.759/–0.509

with the SHELXL-93[46] program incorporated in the SHELXTL/PC V 5.03[47] program package. All non-hydrogen atoms were refined anisotropically. The hydrogen atoms were assigned isotropic displacement factors and included in the final refinement cycles by use of geometrical restraints (C_{ar}–H = 0.93 Å; C_{Me}–H = 0.96 Å; O–H = 0.82 Å). Progams used for molecular plots: XP[47] and MERCURY.[48] CCDC-677255 (**1**), -677256 (**2**), -677257 (**3**) contain the supplementary crystallographic data for this paper. These data can be obtained free of charge from The Cambridge Crystallographic Data Centre via www.ccdc.cam.ac.uk/data_request/cif.

Acknowledgments

This research was financially supported by the Department of Chemistry, University of Louisiana at Lafayette and partially supported by Comisión Interministerial de Ciencia y Tecnología (CICYT) (Grant BQU2003-00538 to R. V.). S. S. M. thanks Dr. R. D. Braun (ULL) and Dean B. Clark, and F. A. M. thanks Dr. J. Baumgartner (TU Graz) for assistance.

---

[1] R. Vicente, E. Ruiz, J. Cano, S. S. Massoud, F. A. Mautner, *Inorg. Chem.* **2008**, DOI: 10.1021/ic/702324q.

[2] S. S. Massoud, F. A. Mautner, R. Vicente, J. S. Dickens, *Inorg. Chim. Acta* **2008**, *361*, 299–308.

[3] L. Soto, N. Ruiz, H. Núñez, J. Server-Carrió, E. Escrivà, A. Sancho, J. Gracía-Lozano, *Inorg. Chim. Acta* **2006**, *359*, 3221–3228.

[4] D. Cangussu, H. O. Stumpf, H. Adams, J. H. Thomas, F. Lloret, M. Julve, *Inorg. Chim. Acta* **2005**, *358*, 2292–2302.

[5] C.-C. Wang, C.-H. Yang, G.-H. Lee, H.-L. Tsai, *Eur. J. Inorg. Chem.* **2005**, 1334–1342.

[6] R. Kirchmaier, E. Altin, A. Lentz, *Z. Kristallogr. – New Cryst. Struct.* **2003**, *218*, 541–542.

[7] Y. Akhriff, J. Server-Carrió, A. Sancho, J. Garcia-Lozano, E. Escrivá, L. Soto, *Inorg. Chem.* **2001**, *40*, 6832–6840.

[8] E. Krupicka, A. Lentz, *Z. Kristallogr. – New Cryst. Struct.* **2001**, *216*, 287–288.

[9] E. Krupicka, A. Lentz, *Z. Kristallogr. – New Cryst. Struct.* **2001**, *216*, 289–290.

[10] I. Castro, M. L. Calatayud, J. Sletten, F. Lloret, M. Julve, *Inorg. Chim. Acta* **1999**, *287*, 173–180.

[11] C.-R. Lee, C.-C. Wang, K.-C. Chen, G.-H. Lee, Y. Wang, *J. Phys. Chem. A* **1999**, *103*, 156–165.

[12] B. D. Alleyne, L. A. Hall, H.-A. Hosein, H. Jaggernauth, A. J. P. White, D. J. Williams, *J. Chem. Soc., Dalton Trans.* **1998**, 3845–3850.

[13] I. Castro, M. L. Calatayud, J. Sletten, F. Lloret, M. Julve, *J. Chem. Soc., Dalton Trans.* **1997**, 811–817.

[14] Z.-H. Zhang, H.-L. Yang, Y. Tang, Z.-H. Ma, Z.-A. Zhu, *Transition Met. Chem.* **2004**, *29*, 590–595.

[15] P. S. Mukherjee, S. Konar, E. Zangrando, C. Diaz, J. Ribas, P. S. Chaudhuri, *J. Chem. Soc., Dalton Trans.* **2002**, 3471–3476.

[16] C. E. Xanthopoulos, M. P. Sigalas, G. A. Katsoulos, C. A. Tsipis, C. C. Hajikostas, A. Terzis, M. Mentzafos, *Inorg. Chem.* **1993**, *32*, 3743–3747.

[17] M. Graf, H. Stoeckli-Evans, A. Escuer, R. Vicente, *Inorg. Chim. Acta* **1997**, *257*, 89–97.

[18] X. Solans, M. Aguilló, A. Gleizes, J. Faus, M. Julve, M. Verdaguer, *Inorg. Chem.* **1990**, *29*, 775–784.

[19] I. Castro, J. Sletten, M. L. Calatayud, M. Julve, J. Cano, F. Lloret, A. Caneschi, *Inorg. Chem.* **1995**, *34*, 4903–4909.

[20] A. Bencini, A. Bianchi, E. Garcia-España, Y. Jeannin, M. Julve, V. Marcelino, M. Philoche-Levisalles, *Inorg. Chem.* **1990**, *29*, 963–970.

[21] R. Soules, F. Dahan, F. J.-P. Laurent, P. Castan, *J. Chem. Soc., Dalton Trans.* **1988**, 587–590.

[22] J. A. C. van Ooijen, J. Reedijk, A. L. Spek, *Inorg. Chem.* **1979**, *18*, 1184–1189.

[23] J. T. Reinprecht, J. G. Miller, G. C. Vogel, M. S. Haddad, D. N. Hendrickson, *Inorg. Chem.* **1980**, *19*, 927–993.

[24] S. Youngme, P. Gunnasoot, P. Narongsak, C. Pakawatchai, *Transition Met. Chem.* **2004**, *29*, 840.

[25] S. C. Manna, A. Zangrando, J. Ribas, N. R. Chaudhuri, *Inorg. Chim. Acta* **2005**, *358*, 4497–4504.

[26] D. M. Duggan, E. K. Barefield, D. N. Hendrickson, *Inorg. Chem.* **1973**, *12*, 985–991.

[27] R. West, H. J. Niu, *J. Am. Chem. Soc.* **1963**, *85*, 2589–2590.

[28] U. Mukhopadhyay, I. Bernal, S. S. Massoud, F. A. Mautner, *Inorg. Chim. Acta* **2004**, *357*, 3673–3682.

[29] a) F. A. Mautner, S. S. Massoud, *J. Mol. Struct.* **2007**, *871*, 108–113; b) S. S. Massoud, F. A. Mautner, M. A. M. Abu-Youssef, N. M. Shuaib, *Polyhedron* **1999**, *18*, 2061–2067.

[30] B. J. Hathaway, in G. Wilkinson, R. D. Gillard, J. A. McCleverty (Eds.), *Comprehensive Coordination Chemistry*, vol. 5, Pergamon, Press, Oxford, England, **1987**, p. 533.

[31] a) S. S. Massoud, F. A. Mautner, R. Vicente, H. N. Sweeney, *Inorg. Chim. Acta* **2006**, *359*, 1489–1500; b) S. S. Massoud, F. A. Mautner, *Inorg. Chim. Acta* **2005**, *358*, 3334–3340; c) S. S. Massoud, F. A. Mautner, *Inorg. Chem. Commun.* **2004**, *7*, 559–562.

[32] M. Schatz, M. Becker, F. Thaler, F. Hampel, S. Schindler, R. R. Jacobson, Z. Tyeklár, N. N. Murthy, P. Ghodh, Q. Chen, J. Zubieta, K. D. Karlin, *Inorg. Chem.* **2001**, *40*, 2312–2322.

[33] a) S. S. Massoud, F. A. Mautner, R. Vicente, B. M. Rodrigue, *Inorg. Chim. Acta* **2006**, *359*, 3321–3329; b) S. S. Massoud, F. A. Mautner, R. Vicente, *Asian Chem. Lett.* **2007**, *11*, 81–92.

[34] G. J. Long, *Inorg. Chem.* **1978**, *17*, 2702–2707.

[35] J. T. Wrobleski, D. Brown, *Inorg. Chem.* **1978**, *17*, 2959–2961.

[36] C. G. Pierpont, L. C. Francesconi, D. N. Hendrickson, *Inorg. Chem.* **1977**, *16*, 2367–2376.

[37] S. S. Massoud, K. T. Broussard, F. A. Mautner, R. Vicente, M. K. Saha, I. Bernal, *Inorg. Chim. Acta* **2008**, *361*, 123–131.

[38] K. D. Karlin, J. C. Hayes, S. Juen, J. P. Hutchinson, J. Zubieta, *Inorg. Chem.* **1982**, *21*, 4106–4108.

[39] S. S. Massoud, F. A. Mautner, R. Vicente, A. A. Gallo, E. Ducasse, *Eur. J. Inorg. Chem.* **2007**, 1091–1102.

[40] A. W. Addison, T. N. Rao, J. Reedijk, J. V. Rijin, G. C. Verschoor, *J. Chem. Soc., Dalton Trans.* **1984**, 1349–1356.

[41] a) C. Robl, W. F. Kuhs, *J. Solid State Chem.* **1988**, *73*, 172–178; b) C. Robl, W. F. Kuhs, *J. Solid State Chem.* **1988**, *75*, 15–20; c) C. Robl, A. Weiss, *Mat. Res. Bull.* **1987**, *22*, 373–380; d) C. Robl, V. Gnutzmann, A. Weiss, *Z. Anorg. Allg. Chem.* **1987**, *549*, 187–194; e) A. Weiss, E. Riegler, I. Alt, H. Böhme, C. Robl, *Z. Naturforsch., Teil B* **1986**, *41*, 18–24; f) C. Robl, A. Weiss, *Z. Naturforsch., Teil B* **1986**, *41*, 1341–1345; g) C. Robl, A. Weiss, *Z. Naturforsch., Teil B* **1986**, *41*, 1485–1489; h) C. Robl, A. Weiss, *Z. Naturforsch., Teil B* **1986**, *41*, 1490–1494; i) C. Robl, A. Weiss, *Z. Naturforsch., Teil B* **1988**, *43b*, 99–103.

[42] G. Anderegg, F. Wenk, *Helv. Chim. Acta* **1967**, *50*, 2330.

[43] J. Mukherjee, V. Balamurugan, R. Gupta, R. Mukherjee, *Dalton Trans.* **2003**, 3686–3692.

[44] R. H. Blessing, *Acta Crystallogr., Sect. A* **1995**, *51*, 33–38; SADABS: Bruker AXS, **1998**.

[45] G. M. Sheldrick, *SHELXS-86: Program for the Solution of Crystal Structure*, University of Göttingen, Göttingen, Germany, **1986**.

[46] G. M. Sheldrick, *SHELXL-93: Program for the Refinement of Crystal Structure*, University of Göttingen, Göttingen, Germany, **1993**.

[47] *SHELXTL 5.03 (PC-Version)*, Program Library for the Solution and Molecular Graphics, Siemens Analytical Instruments Division, Madison, WI, **1995**.

[48] MERCURY, version 1.4.1, available at CCDC, http://www.ccdc.cam.ac.uk/mercury/.

Received: February 17, 2008